

Some Case Studies Using Bayesian Statistical Models

Juan Sosa, Universidad Nacional, Colombia*
Lina Buitrago, Universidad Nacional, Colombia†

Abstract

We provide four case studies that use Bayesian machinery to making inductive reasoning. Our main motivation relies in offering several instances where the Bayesian approach to data analysis is exploited at its best to perform complex tasks, such as description, testing, estimation, and prediction. This work is not meant to be either a reference text or a survey in Bayesian statistical inference. Our goal is simply to provide several examples that use Bayesian methodology to solve data-driven problems. The topics we cover here, include problems in Bayesian nonparametrics, Bayesian analysis of times series, and Bayesian analysis of spatial data.

Keywords: Bayesian Models. Gibbs Sampler. Hierarchical Models. Markov chain Monte Carlo. Statistical Inference.

1 Introduction

In this manuscript, we provide four case studies that use Bayesian machinery to making inductive reasoning. Our main motivation relies in offering several instances where the Bayesian approach to data analysis is exploited at its best to perform complex tasks, such as description (probabilistic summary of main data patterns), testing (evaluation of competing theories of data formation), estimation (evaluation of parameters in a presumed model), and prediction (forecast of missing or future observations).

We focus on model-based approaches to perform statistical inference. In particular, our case studies are totally based on Bayesian statistics. A statistical model fully describes

*jcsosam@unal.edu.co

†labuitragor@unal.edu.co

the data generating process under which a given dataset might have arisen. Thus, the vector of observations $\mathbf{y} = (y_1, \dots, y_n)$ is assumed to be generated by an unknown probability distribution P with probability density/mass function p . Therefore, we have that all information in the data is contained in P .

Furthermore, in Bayesian statistics we treat the model parameters that index P , $\boldsymbol{\theta} = (\theta_1, \dots) \in \Theta$, as random variables, which in turn are assigned a prior distribution Π with probability density/mass function p (even though it is an abuse of mathematical notation, since the probability density/mass function associated with P is also denoted with p). The prior distribution captures the uncertainty of the researcher about the value of $\boldsymbol{\theta}$ before observing \mathbf{y} (another way to think about the prior is as summarizing all information about $\boldsymbol{\theta}$ that is external to \mathbf{y}).

If we use probability theory to express all forms of uncertainty associated with our statistical model $\mathcal{M} = (p(\mathbf{y} | \boldsymbol{\theta}), p(\boldsymbol{\theta}))$, then Bayes theorem can be used to update our knowledge about $\boldsymbol{\theta}$, through the posterior distribution

$$p(\boldsymbol{\theta} | \mathbf{y}) \propto \frac{p(\mathbf{y} | \boldsymbol{\theta}) p(\boldsymbol{\theta})}{\int_{\Theta} p(\mathbf{y} | \boldsymbol{\theta}) p(\boldsymbol{\theta}) d\boldsymbol{\theta}}.$$

The posterior combines information in the data with any other information external to it that has been encoded in the prior. Again, we slightly abuse notation by using p to denote the distribution of $\mathbf{y} | \boldsymbol{\theta}$ as well as that of $\boldsymbol{\theta} | \mathbf{y}$.

The Bayesian approach is convenient for several reasons. First of all, in a Bayesian setting all forms of uncertainty quantification are granted. Moreover, it is natural to think about hierarchies, and therefore, borrowing of information (hierarchical models are used in non-Bayesian approaches, but they are not as natural). Also, with the advent of Markov chain Monte Carlo (MCMC) and other simulation-based approaches, computation has become in some ways easier than computation for non-Bayesian approaches (particularly for complex models). Lastly, since both observations and parameters are random variables, dealing with missing and censored data is simpler.

This work is not meant to be either a reference text or a survey in Bayesian statistical inference. Our goal is simply to provide several examples that use Bayesian methodology to solve data-driven problems. Therefore, we expect that the reader has a working understating of Bayesian methods for model building and computation. For a deep treatment of Bayesian data analysis methods, we refer the reader to Gelman et al. (2014), Robert (2007), Jackman (2009), among many others. Finally, the topics we cover here, include problems in Bayesian nonparametrics (e.g., Müller et al. 2015), Bayesian analysis of times series (e.g., Prado and West 2010), and Bayesian analysis of spatial data (e.g., Banerjee et al. 2014).

The rest of the document is structured as follows: Section 2 presents an example using synthetic data in the context of nonparametric regression; Section 3 offers the analysis of a time series using dynamic linear models; Section 4 provides an illustration of a space-time model for areal unit data; Section 5 exhibits a case regarding species sampling models; finally, Section 6 gives a brief discussion.

2 Nonparametric regression modeling

Consider the Gaussian process (GP) regression setting (e.g., Taddy and Kottas 2010) with a single continuous covariate,

$$y_i = f(x_i) + \epsilon_i, \quad i = 1, \dots, n, \quad (1)$$

where y_i and x_i are the response and covariate observations, respectively, ϵ_i are independent and identically distributed (iid) random errors from a $\mathbf{N}(0, \sigma^2)$ distribution, and $f(\cdot)$ is the regression function, which is assigned a GP prior with constant mean function $\mathbf{E}(f(x) \mid \mu) = \mu$, and power exponential covariance function $\text{Cov}(f(x), f(x') \mid \tau, \phi) = \tau^2 \exp\{-\phi|x - x'|^\alpha\}$, with unknown $\tau > 0$ and $\phi > 0$, but fixed $0 < \alpha \leq 2$ (the special cases for $\alpha = 1$ and $\alpha = 2$ correspond to the Exponential and Gaussian covariance functions, respectively). Here, α defines the smoothness of the function, τ^2 determines the amplitude of oscillation, and ϕ delimits the volatility of orientation. Lastly, recall that based on the GP definition, for any collection of index points t_1, \dots, t_n , the random vector $(x_{t_1}, \dots, x_{t_n})$ follows an n -variate Normal distribution with mean vector $(\mu(t_1), \dots, \mu(t_n))$, and positive definite covariance matrix whose (i, j) -th element is given by $\text{Cov}(x_{t_i}, x_{t_j}) = \tau^2 \exp\{-\phi|t_i - t_j|^\alpha\}$.

In order to perform full Bayesian inference under this setting, we consider the following independent prior distributions for the remaining model parameters:

$$\sigma^2 \sim \text{IG}(a_\sigma, b_\sigma), \quad \mu \sim \mathbf{N}(a_\mu, b_\mu), \quad \tau^2 \sim \text{IG}(a_\tau, b_\tau), \quad \phi \sim \text{U}(a_\phi, b_\phi).$$

Note that by letting $\boldsymbol{\theta} = (\theta_1, \dots, \theta_n)$, with $\theta_i = f(x_i)$ for $i = 1, \dots, n$, denote the unknown function values, it follows that $\mathbf{y} \mid \boldsymbol{\theta}, \sigma^2 \sim \mathbf{N}_n(\boldsymbol{\theta}, \sigma^2 \mathbf{I})$ and $\boldsymbol{\theta} \mid \boldsymbol{\mu}, \mathbf{H} \sim \mathbf{N}_n(\boldsymbol{\mu}, \mathbf{H})$, with $\mathbf{y} = (y_1, \dots, y_n)$, $\boldsymbol{\mu} = \mu \mathbf{1}$ and $\mathbf{H} = \tau^2 \mathbf{C}$, where $\mathbf{C} = [\exp\{-\phi|x_i - x_j|^\alpha\}]$, which means that once $\boldsymbol{\theta}$ has been integrated out $\mathbf{y} \mid \boldsymbol{\mu}, \sigma^2, \mathbf{H} \sim \mathbf{N}_n(\boldsymbol{\mu}, \sigma^2 \mathbf{I} + \mathbf{H})$.

Now, we provide a Gibbs sampling algorithm designed to draw samples from the posterior distribution

$$p(\boldsymbol{\Upsilon} \mid \mathbf{y}) \propto p(\mathbf{y} \mid \boldsymbol{\theta}, \sigma^2) p(\boldsymbol{\theta} \mid \boldsymbol{\mu}, \mathbf{H}) p(\mu) p(\sigma^2) (\tau^2) p(\phi),$$

where $\boldsymbol{\Upsilon} = (\boldsymbol{\theta}, \sigma^2, \mu, \tau^2, \phi)$. Let $\boldsymbol{\Upsilon}^{(b)}$ be the vector of model parameters at iteration b of the algorithm, for $b = 1, \dots, B$. Given a starting point $\boldsymbol{\Upsilon}^{(0)}$, we consider a Gibbs sampler (with a Metropolis step) updating $\boldsymbol{\Upsilon}^{(b-1)}$ to $\boldsymbol{\Upsilon}^{(b)}$ until convergence as follows:

1. Sample $\boldsymbol{\theta} \mid \sigma^2, \mu, \tau^2, \phi, \mathbf{y} \sim \mathbf{N}_n(\mathbf{m}_\theta, \mathbf{V}_\theta)$, with

$$\mathbf{V}_\theta = (\sigma^{-2}\mathbf{I} + \mathbf{H}^{-1})^{-1} \quad \text{and} \quad \mathbf{m}_\theta = \mathbf{V}_\theta (\sigma^{-2}\mathbf{y} + \mathbf{H}^{-1}\boldsymbol{\mu}) .$$

2. Sample $\sigma^2 \mid \boldsymbol{\theta} \sim \text{IG}(a_\sigma + \frac{n}{2}, b_\sigma + \frac{1}{2} \sum_{i=1}^n (y_i - \theta_i)^2)$.

3. Sample $\mu \mid \boldsymbol{\theta}, \tau^2, \phi \sim \mathbf{N}(m_\mu, V_\mu)$, with

$$V_\mu = (b_\mu^{-1} + \mathbf{1}^\top \mathbf{H}^{-1} \mathbf{1})^{-1} \quad \text{and} \quad m_\mu = V_\mu [a_\mu b_\mu^{-1} + \mathbf{1}^\top \mathbf{H}^{-1} \boldsymbol{\theta}] .$$

4. Sample $\tau^2 \mid \boldsymbol{\theta}, \mu, \phi \sim \text{IG}(a_\tau + \frac{n}{2}, b_\tau + \frac{1}{2}(\boldsymbol{\theta} - \boldsymbol{\mu})^\top \mathbf{C}^{-1}(\boldsymbol{\theta} - \boldsymbol{\mu}))$.

5. Sample ϕ using a Metropolis step:

- a. Set $\eta = \text{logit}((\phi - a_\phi)/(b_\phi - a_\phi))$.

- b. Sample $\eta^* \sim \mathbf{N}(\eta, \delta)$, with δ a tuning parameter.

- c. Compute $r = \exp\{\log p_\eta(\eta^* \mid \boldsymbol{\theta}, \mu, \tau^2) - \log p_\eta(\eta \mid \boldsymbol{\theta}, \mu, \tau^2)\}$, with

$$\log p_\eta(x \mid \boldsymbol{\theta}, \mu, \tau^2) = \frac{1}{2} (\log |\mathbf{H}^{-1}| - (\boldsymbol{\theta} - \boldsymbol{\mu})^\top \mathbf{H}^{-1}(\boldsymbol{\theta} - \boldsymbol{\mu})) + x - 2 \log(1 + e^x) + k ,$$

where k is a constant.

- d. Update ϕ to $\phi^* = (b_\phi - a_\phi)\text{expit}(\eta^*) + a_\phi$ with probability r .

Now, in order to test the previous algorithm, we generate synthetic data according to model (1) with $\sigma = 0.2$, $x_i \stackrel{\text{iid}}{\sim} \text{U}(-3, 3)$, for $i = 1, \dots, 100$, and the true regression function $f(x) = 0.3 + 0.4x + 0.5 \sin(2.7x) + \frac{1.1}{1+x^2}$ (this example is included in a technical report by Radford Neal, which is available on-line from <http://www.cs.toronto.edu/~radford/mc-gp.abstract.html>). Panel (a) in Figure 1 shows the simulated dataset. Here, we adopt an empirical Bayes approach by setting $a_\mu = \bar{y}$, $a_\sigma = a_\tau = 2$, $b_\mu = b_\sigma = b_\tau = s_y^2/3$, since marginally $\mathbf{E}(y_i) = a_\mu = \bar{y}$ and $\text{Var}(y_i) = b_\mu + b_\sigma + b_\tau = s_y^2$; and also, $a_\phi = 0.1$ and $b_\phi = 10$, which let ϕ vary across a wide range of values. Thus, we fit the model with $\alpha = 1$ and run the algorithm choosing δ (step 5.) carefully to produce a reasonable average mixing rate between 30% and 50%.

The results presented below are based on $B = 25000$ samples from the posterior distribution $p(\boldsymbol{\Upsilon} \mid \mathbf{y})$ obtained after thinning the original chain every 10 observations and

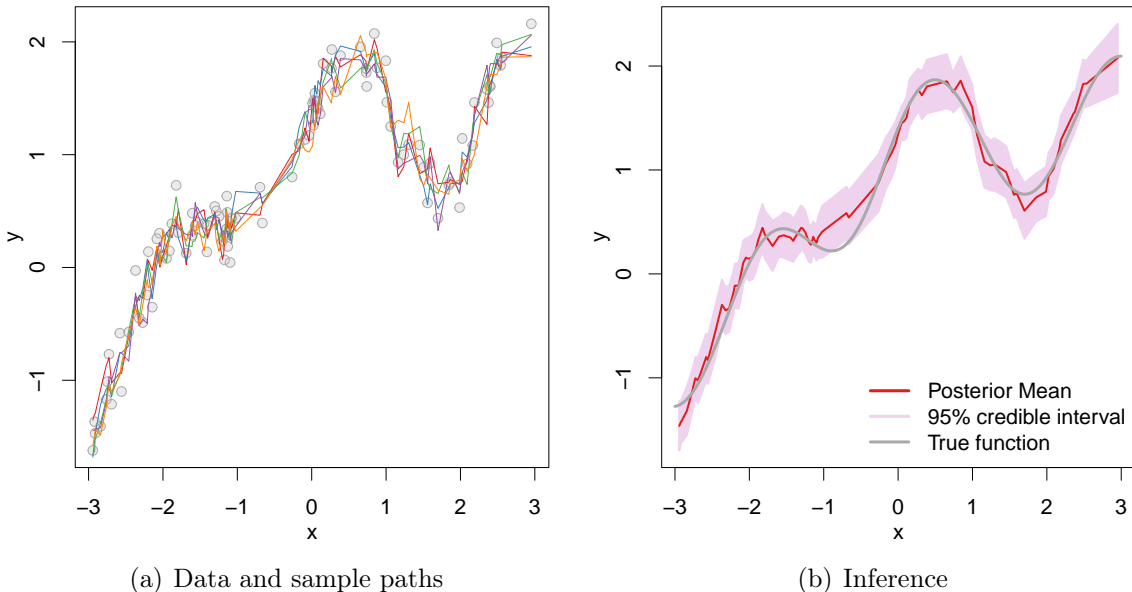


Figure 1: Data along with five sample paths chosen at random from the posterior distribution of θ , and posterior inference on $f(\cdot)$.

a burn-in period of 5000 iterations. Chains mixed reasonably well and effective sample sizes for θ range from 22921 to 26436. Panel (a) in Figure 1 shows five sample paths chosen at random from the posterior distribution of θ . We see how these paths fit very well to the data. On the other hand, Table 1 summarizes the posterior distribution of σ^2 , μ , τ^2 , and ϕ . Note that the 95% quantile-based credible interval for σ^2 includes the true value (0.04). Finally, Panel (b) in Figure 1 shows the posterior mean along with 95% credible intervals for $f(\cdot)$. Almost the entire true function falls within the credible bands, which shows that the model specification as well as the prior elicitation was suitable in this case.

Parameter	Mean	SD	2.5%	50%	97.5%
σ^2	0.0334	0.0063	0.0228	0.0327	0.0476
μ	0.6117	0.3932	-0.1654	0.6144	1.3862
τ^2	0.8075	0.4035	0.3303	0.7009	1.8700
ϕ	0.3590	0.1740	0.1200	0.3296	0.7710

Table 1: Posterior summaries for σ^2 , μ , τ^2 , and ϕ .

3 Dynamic linear modeling

Figure 2 shows the detrended zero-centered weekly change series y_1, \dots, y_T associated with the U.S. 3-year Treasury Constant Maturity Interest Rate from March 18, 1988 to September 10, 1999. We have $T = 600$ equally spaced measurements in total. This series does not exhibit additional trends and seems to be stationary (which is confirmed below), so we do not differentiate the data again.

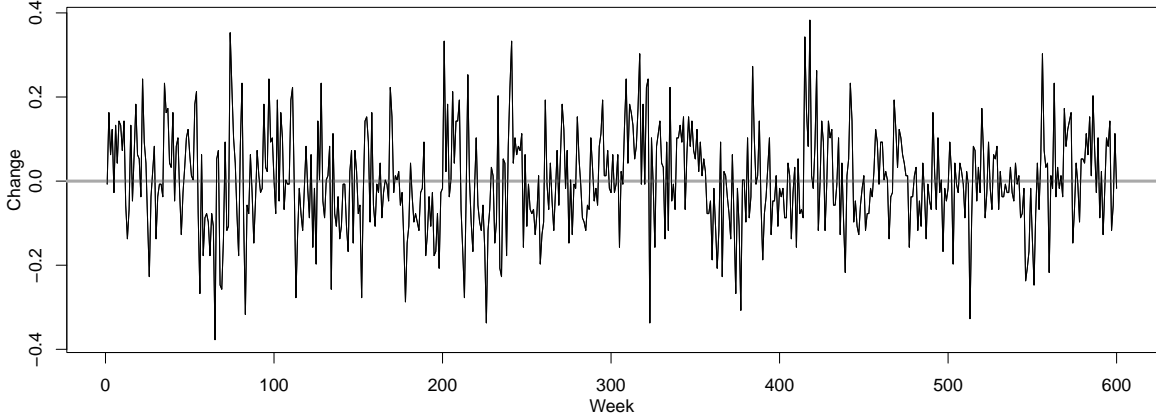


Figure 2: Detrended zero-centered weekly change series of the U.S. 3-year Treasury Constant Maturity Interest Rate from March 18, 1988 to September 10, 1999.

3.1 Autoregressive model

As a naive analysis of the series, we consider a model of the form

$$y_t = \phi_1 y_{t-1} + \dots + \phi_p y_{t-p} + \epsilon_t, \quad \epsilon_t | v \stackrel{\text{iid}}{\sim} \mathbf{N}(0, v), \quad (2)$$

which corresponds to an autoregressive model of order p , $\text{AR}(p)$. We fit this model to the data using a reference prior distribution of the form $p(\boldsymbol{\phi}, v) \propto 1/v$, with $\boldsymbol{\phi} = (\phi_1, \dots, \phi_p)$, and the conditional likelihood

$$p(\mathbf{y} | y_1, \dots, y_p, \boldsymbol{\phi}, v) = \prod_{t=p+1}^T \mathbf{N}(y_t | \mathbf{f}_t^\top \boldsymbol{\phi}, v) = \mathbf{N}_{T-p}(\mathbf{y} | \mathbf{F}^\top \boldsymbol{\phi}, v\mathbf{I}) \quad (3)$$

where $\mathbf{y} = (y_{p+1}, \dots, y_T)$ since the first p observations are considered as initial values, $\mathbf{f}_t = (y_{t-1}, \dots, y_{t-p})$ for $t = p + 1, \dots, T$, and $\mathbf{F} = [\mathbf{f}_{p+1}, \dots, \mathbf{f}_T]$. This formulation corresponds to a regular linear model setting, and therefore, we can apply standard theory (Prado and West, 2010, pp. 19-22).

Combining the likelihood (3) with the prior distribution $p(\boldsymbol{\phi}, v)$, we can easily obtain samples from the posterior distribution $p(\boldsymbol{\phi}, v \mid \mathbf{y})$ using direct sampling as follows: first, sample v from $\text{IG}((n-p)/2, (n-p)\hat{v}^2/2)$, and then, for each v in the previous step sample $\boldsymbol{\phi}$ from a $\text{N}_p(\hat{\boldsymbol{\phi}}_{\text{mle}}, v(\mathbf{F}\mathbf{F}^\top)^{-1})$. Using $p = 3$, it follows that $n = T - p = 597$, $(n-p)\hat{v}^2 = 7.6759$ is the residual sum of squares, which in turn leads to $\hat{v}_{\text{mle}} = 0.0128$ the MLE of v , and $\hat{\boldsymbol{\phi}}_{\text{mle}} = (\mathbf{F}\mathbf{F}^\top)^{-1}\mathbf{F}\mathbf{y} = (0.2283, 0.0018, 0.1146)$ is the MLE of $\boldsymbol{\phi}$. Posterior summaries of 25000 samples from $p(\boldsymbol{\phi}, v \mid \mathbf{y})$ are provided in Table 2. We see that the posterior parameter estimates are very similar to their MLE counterpart.

Parameter	Mean	SD	2.5%	50%	97.5%
ϕ_1	0.2267	0.0407	0.1462	0.2267	0.3066
ϕ_2	0.0063	0.0420	-0.0753	0.0058	0.0896
ϕ_3	0.1132	0.0408	0.0334	0.1132	0.1936
v	0.0130	0.0007	0.0116	0.0129	0.0145

Table 2: Posterior summaries for $\boldsymbol{\phi}$ and v .

3.2 Dynamic linear model

Now, going forward in the analysis, we consider a popular model given in (Tsay, 2010, p. 561) for detecting outliers:

$$\begin{aligned}
 y_t &= \gamma_t \alpha_t + x_t + \epsilon_t, & \gamma_t &\stackrel{\text{iid}}{\sim} \text{Ber}(0.2), & \alpha_t &\stackrel{\text{iid}}{\sim} \text{N}(0, 0.1), & \epsilon_t &\stackrel{\text{iid}}{\sim} \text{N}(0, 0.01), \\
 x_t &= \phi_1 x_{t-1} + \dots + \phi_p x_{t-p} + \eta_t, & \eta_t &| \omega &\stackrel{\text{iid}}{\sim} \text{N}(0, \omega).
 \end{aligned}
 \tag{4}$$

Under this formulation, γ_t denotes the presence or absence of an additive outlier at time t , and α_t its corresponding magnitude when present, and. Thus, additive outliers are allowed to occur at every time point with a probability equal to 0.2. Furthermore, x_t defines an autoregressive process with order p . Then, we have $3T + p + 1$ model parameters, namely, $\boldsymbol{\gamma} = (\gamma_1, \dots, \gamma_T)$, $\boldsymbol{\alpha} = (\alpha_1, \dots, \alpha_T)$, $\mathbf{x} = (x_1, \dots, x_T)$, $\boldsymbol{\phi} = (\phi_1, \dots, \phi_p)$, and ω . Also, we also assume the conjugate priors $\phi_j \stackrel{\text{iid}}{\sim} \text{N}(a_\phi, b_\phi)$, for $j = 1, \dots, p$, and $\omega \sim \text{IG}(a_\omega, b_\omega)$.

Note that model (4) is a non-Gaussian dynamic linear model (DLM). However, conditional on the outlier indicators γ_t , this model can be written as a standard DLM. For instance, with $p = 3$ the model acquires the form:

$$\begin{aligned}
 y_t &= \mathbf{F}^\top \boldsymbol{\theta}_t + \nu_t, & \nu_t &| V_t \stackrel{\text{ind}}{\sim} \text{N}(0, V_t), \\
 \boldsymbol{\theta}_t &= \mathbf{G} \boldsymbol{\theta}_{t-1} + \boldsymbol{\omega}_t, & \boldsymbol{\omega}_t &| \mathbf{W}_t \stackrel{\text{ind}}{\sim} \text{N}_p(\mathbf{0}, \mathbf{W}_t),
 \end{aligned}
 \tag{5}$$

with

$$\mathbf{F} = (1, 0, 0), \quad \boldsymbol{\theta}_t = (x_t, x_{t-1}, x_{t-2}), \quad V_t = v_{\gamma_t} = \begin{cases} 0.01, & \gamma_t = 0; \\ 0.11, & \gamma_t = 1, \end{cases}$$

and

$$\mathbf{G} = \begin{pmatrix} \phi_1 & \phi_2 & \phi_3 \\ 1 & 0 & 0 \\ 0 & 1 & 0 \end{pmatrix}, \quad \boldsymbol{\omega}_t = (\eta_t, 0, 0), \quad \mathbf{W}_t = \mathbf{W} = \begin{pmatrix} \omega & 0 & 0 \\ 0 & 0 & 0 \\ 0 & 0 & 0 \end{pmatrix}.$$

We use the previous fact to develop the second step of the MCMC algorithm described below. There, we implement a forward filtering backward sampling algorithm (Prado and West, 2010, p. 137) to get samples from $p(\boldsymbol{\theta}_{1:T} \mid \boldsymbol{\gamma}, \boldsymbol{\phi}, \omega)$, which automatically allow us to draw samples from $p(\mathbf{x} \mid \boldsymbol{\gamma}, \boldsymbol{\phi}, \omega)$.

Now, we describe the general form of the MCMC to obtain samples from the posterior distribution

$$p(\boldsymbol{\Upsilon} \mid \mathbf{y}) \propto p(\mathbf{y} \mid \boldsymbol{\gamma}, \boldsymbol{\alpha}, \mathbf{x}) p(\mathbf{x} \mid \boldsymbol{\phi}, \omega) p(\boldsymbol{\gamma}) p(\boldsymbol{\alpha}) p(\boldsymbol{\phi}) p(\omega),$$

where $\boldsymbol{\Upsilon} = (\boldsymbol{\gamma}, \boldsymbol{\alpha}, \mathbf{x}, \boldsymbol{\phi}, \omega)$ and $\mathbf{y} = (y_1, \dots, y_T)$. Full conditional distributions are derived looking at the dependencies in $p(\boldsymbol{\Upsilon} \mid \mathbf{y})$. Let $\boldsymbol{\Upsilon}^{(b)}$ be the vector of model parameters at iteration b of the algorithm, for $b = 1, \dots, B$. Given a starting point $\boldsymbol{\Upsilon}^{(0)}$, we consider a Gibbs sampler (with a FFBS step) updating $\boldsymbol{\Upsilon}^{(b-1)}$ to $\boldsymbol{\Upsilon}^{(b)}$ until convergence as follows:

1. Sample $\alpha_t \mid \theta_{t,1}, \gamma_t, y_t \sim \mathbf{N}(m_t, V_t)$, for $t = 1, \dots, T$, with

$$V_t = \frac{1}{10(10\gamma_t + 1)} \quad \text{and} \quad m_t = 100V_t\gamma_t(y_t - \theta_{t,1}).$$

2. Sample $\gamma_t \mid \theta_{t,1}, y_t \sim \text{Ber}(p_t)$, for $t = 1, \dots, T$, with

$$\frac{p_t}{1 - p_t} = \frac{1}{4\sqrt{11}} \exp \left\{ -\frac{1}{2}(y_t - \theta_{t,1})^2(1/0.11 - 1/0.01) \right\}.$$

3. Sample $\boldsymbol{\phi} \mid \boldsymbol{\theta}_{1:T}, \omega \sim \mathbf{N}_p(\mathbf{m}_\phi, \mathbf{V}_\phi)$, with

$$\mathbf{V}_\phi = \left(b_\phi^{-1} \mathbf{I} + \frac{1}{\omega} \sum_{t=1}^T \boldsymbol{\theta}_{t-1} \boldsymbol{\theta}_{t-1}^\top \right)^{-1} \quad \text{and} \quad \mathbf{m}_\phi = \mathbf{V}_\phi \left(a_\phi b_\phi^{-1} \mathbf{1} + \frac{1}{\omega} \sum_{t=1}^T \theta_{t,1} \boldsymbol{\theta}_{t-1} \right).$$

4. Sample $\omega \mid \boldsymbol{\theta}_{1:T}, \boldsymbol{\phi} \sim \text{IG}(A_\omega, B_\omega)$, with

$$A_\omega = a_\omega + \frac{T}{2} \quad \text{and} \quad B_\omega = b_\omega + \frac{1}{2} \sum_{t=1}^T (\theta_{t,1} - \boldsymbol{\phi}^\top \boldsymbol{\theta}_t)^2.$$

5. Sample $\boldsymbol{\theta}_t$, for $t = 1, \dots, T$, using a FFBS step. Here we use standard DLM notation, in particular that corresponding to the Kalman filter (West and Harrison, 1999, Theorem 4.1, pp. 103-105):

a. Use the filter equations to compute \mathbf{a}_t , \mathbf{R}_t , \mathbf{m}_t , and \mathbf{C}_t , for $t = 1, \dots, T$:

$$\mathbf{a}_t = \mathbf{G}_t \mathbf{m}_{t-1}, \quad \mathbf{R}_t = \mathbf{G}_t \mathbf{C}_{t-1} \mathbf{G}_t^\top + \mathbf{W}_t, \quad \mathbf{m}_t = \mathbf{a}_t + \mathbf{A}_t e_t, \quad \mathbf{C}_t = \mathbf{R}_t - Q_t \mathbf{A}_t \mathbf{A}_t^\top,$$

with $e_t = y_t - f_t$, $f_t = \mathbf{F}_t^\top \mathbf{a}_t$, and $Q_t = \mathbf{F}_t^\top \mathbf{R}_t \mathbf{F}_t + V_t$.

b. At time $t = T$, sample $\boldsymbol{\theta}_T \sim \text{N}_p(\mathbf{m}_T, \mathbf{C}_T)$.

c. For $t = (T-1), \dots, 0$, sample $\boldsymbol{\theta}_t \sim \text{N}(\mathbf{m}_t^*, \mathbf{C}_t^*)$, where

$$\mathbf{m}_t^* = \mathbf{m}_t + \mathbf{B}_t (\boldsymbol{\theta}_{t+1} - \mathbf{a}_{t+1}) \quad \text{and} \quad \mathbf{C}_t^* = \mathbf{C}_t - \mathbf{B}_t \mathbf{R}_{t+1} \mathbf{B}_t^\top,$$

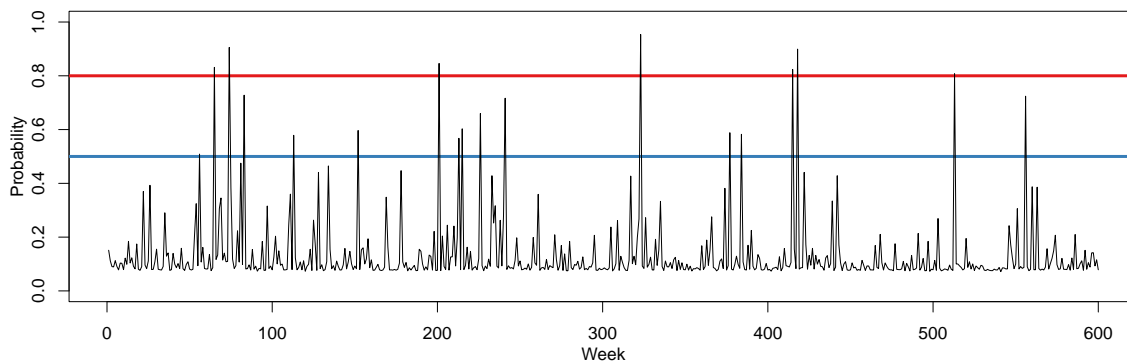
with $\mathbf{B}_t = \mathbf{C}_t \mathbf{G}_{t+1}^\top \mathbf{R}_{t+1}^{-1}$.

Now, we implement the MCMC provided above. To do so, we need to choose appropriate values for a_ϕ , b_ϕ , a_ω , and b_ω . First, $a_\phi = 0$ and $b_\phi = 0.25$ are reasonable values in accordance with our introductory analysis of the series using a standard autoregressive model. On the other hand, we weakly concentrate the prior distribution of ω around $\hat{v}_{\text{mle}} = 0.0128$ from our introductory analysis, by setting $a_\omega = 2$ and $b_\omega = \hat{v}_{\text{mle}}$, which leads to $\text{E}(\omega) = \hat{v}_{\text{mle}}$ with infinite variance. The results presented below are based on $B = 25000$ samples from the posterior distribution $p(\boldsymbol{\Upsilon} \mid \mathbf{y})$ obtained after a burn-in period of 5000 iterations. Chains mixed very well and there is no sign of lack of convergence. Effective sample sizes range from 398.7 to 29019.3.

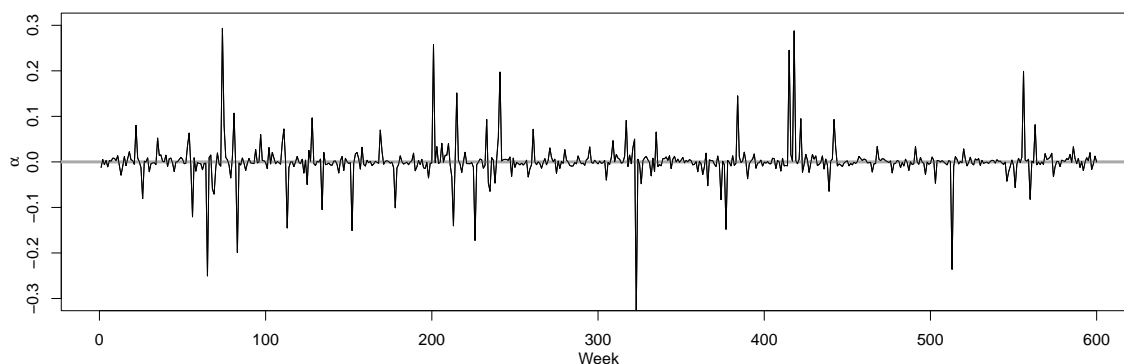
Table 3 display summaries for the posterior distribution of $\boldsymbol{\phi}$ and ω . Estimates for ϕ_3 and ω are consistent with those obtained in Table 2 using a standard autoregressive

Parameter	Mean	SD	2.5%	50%	97.5%
ϕ_1	0.4692	0.1605	0.1618	0.4665	0.7904
ϕ_2	0.1341	0.1932	-0.2694	0.1492	0.4727
ϕ_3	0.1296	0.1367	-0.1495	0.1309	0.4029
ω	0.0017	0.0004	0.0010	0.0016	0.0026

Table 3: Posterior summaries for $\boldsymbol{\phi}$ and ω .



(a) $\Pr(\gamma_t = 1 \mid \mathbf{y})$

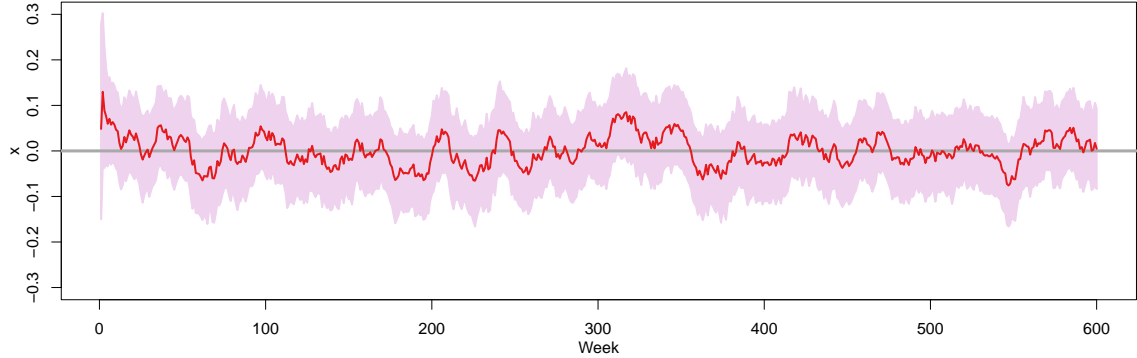


(b) $E(\alpha_t \mid \mathbf{y})$

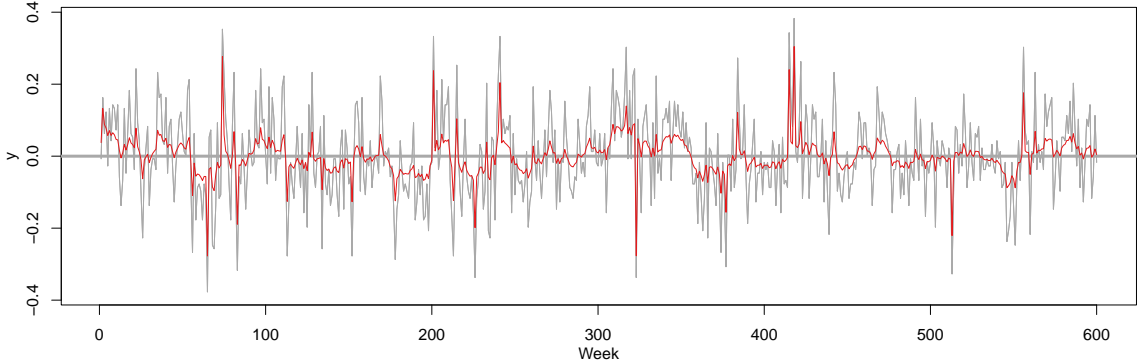
Figure 3: (a) Posterior probability that an observation is an outlier (lines correspond to 0.5 and 0.8). (b) Posterior mean of an outlier size.

model. However, estimates for ϕ_1 and ϕ_2 are utterly different. Such a difference is expected since the autoregressive model does not consider additive outliers, and as a consequence, is not able to characterize fundamental features of the series such as its mean evolution. On the other hand, Figure 3 shows the posterior probability that an observation is an outlier $\Pr(\gamma_t = 1 \mid \mathbf{y})$ along with the corresponding posterior mean of an outlier size $E(\alpha_t \mid \mathbf{y})$, for $t = 1, \dots, T$. We identify 18 observations such that $\Pr(\gamma_t = 1 \mid \mathbf{y}) > 0.5$, seven of which are greater than 0.8, namely, observation at weeks 65, 74, 201, 323, 415, 418, and 513. Tsay (2010, p. 564) also classifies these points as outliers (employing an approach with mild differences) and highlight observations at times $t = 323$ (May 20, 1994) and $t = 201$ (January 17, 1992). At the former, there was a 0.6% drop in the weekly interest rate, while at the later, there was a jump of about 0.35%. Finally, Figure 4 displays the estimated autoregressive process as well as the fitted values along with the original data. We see that the model captures reasonably

well the “volatility” of the series.



(a) $E(x_t | \mathbf{y})$



(b) $E(\gamma_t \alpha_t + x_t | \mathbf{y})$

Figure 4: (a) Posterior inference on the autoregressive process. (b) Data (gray) and fitted values (red).

4 Areal unit space-time modeling

We consider an ecological application in which a spatiotemporal model for areal unit data is considered for modeling a set of binary observations $y_{i,t} = y_t(\mathbf{s}_i)$, for $i = 1, \dots, I$ and $t = 1, \dots, T$, in a discrete time period over a fixed lattice $\mathbf{s}_1, \dots, \mathbf{s}_I$. Here, we consider the Google flu data corresponding to the first 12 weeks of 2013 for the contiguous continental states in the United States (Alaska and Hawaii are omitted from the analysis). Thus, we record a binary variable $y_{i,t}$ that is equal to 1 if the Google flue index for state i during week t is greater than 7500 cases, and 0 otherwise.

We have that the observations $y_{i,t}$ are Bernoulli distributed with probability of success

$\pi_{i,t}$, i.e., $y_{i,t} \mid \pi_{i,t} \sim \text{Ber}(\pi_{i,t})$. Here, we consider the following areal hierarchical generalized linear model (Banerjee et al., 2014, Sec. 6.4) including a temporal component:

$$y_{i,t} \mid \omega_{i,t} = \begin{cases} 1, & \text{if } \omega_{i,t} > 0; \\ 0, & \text{if } \omega_{i,t} \leq 0, \end{cases} \quad (6)$$

$$\omega_{i,t} \mid \boldsymbol{\beta}, \boldsymbol{\gamma}, \xi, \theta_{i,t}, \phi_{i,t}, \kappa_t \stackrel{\text{iid}}{\sim} \text{N}(\mathbf{x}_i^\top \boldsymbol{\beta} + \mathbf{z}_i^\top \boldsymbol{\gamma} + \xi t + \theta_{i,t} + \phi_{i,t}, 1/\kappa_t),$$

with a hierarchical prior distribution of the form

$$\begin{aligned} \beta_k &\stackrel{\text{iid}}{\sim} \text{N}(0, \sigma_0^2), & \gamma_\ell &\stackrel{\text{iid}}{\sim} \text{CAR}(1/\sigma_0^2), & \xi &\sim \text{N}(0, \sigma_0^2), & (7) \\ \theta_{i,t} \mid \tau_t &\stackrel{\text{iid}}{\sim} \text{N}(0, 1/\tau_t), & \phi_{i,t} \mid \lambda_t &\stackrel{\text{iid}}{\sim} \text{CAR}(\lambda_t), & \kappa_t &\stackrel{\text{iid}}{\sim} \text{G}(\nu_0/2, \nu_0/2), \\ \tau_t &\stackrel{\text{iid}}{\sim} \text{G}(a_\tau, b_\tau), & \lambda_t &\stackrel{\text{iid}}{\sim} \text{G}(a_\lambda, b_\lambda), \end{aligned}$$

for $k = 1 \dots, K$, $\ell = 1, \dots, L$, where ν_0 is a fixed positive integer, $\sigma_0^2, a_\tau, b_\tau, a_\lambda, b_\lambda$ are fixed positive real numbers, and $\boldsymbol{\beta} = (\beta_1, \dots, \beta_K)$, $\mathbf{x}_i = \mathbf{x}(\mathbf{s}_i) = (x_1(\mathbf{s}_i), \dots, x_K(\mathbf{s}_i))$, $\boldsymbol{\gamma} = (\gamma_1, \dots, \gamma_L)$, and $\mathbf{z}_i = \mathbf{z}_i(\mathbf{s}_i) = (z_1(\mathbf{s}_i), \dots, z_L(\mathbf{s}_i))$.

The link function $g(\cdot)$ relating the $\pi_{i,t}$ and the linear predictor is based in a Student-t distribution with ν_0 degrees of freedom, which is particularly useful to detect rare events (those with small $\pi_{i,t}$). Since $\omega_{i,t} = \eta_{i,t} + \phi_{i,t} + \epsilon_{i,t}$ with $\eta_{i,t} = \mathbf{x}_i^\top \boldsymbol{\beta} + \mathbf{z}_i^\top \boldsymbol{\gamma} + \xi t + \theta_{i,t}$, $\epsilon_{i,t} \sim \text{N}(0, 1/\kappa_t)$ and $\kappa_t \sim \text{G}(\nu_0/2, \nu_0/2)$, then the marginal distribution of $\epsilon_{i,t}$ (and therefore $\omega_{i,t}$) is Student-t with ν_0 degrees of freedom. Thus, due to the symmetry of the t distribution, we have that $\Pr(y_{i,t} = 1 \mid \omega_{i,t}) = \Pr(\epsilon_{i,t} \leq \eta_{i,t})$, and therefore, $\pi_{i,t} = F_{\nu_0}(\eta_{i,t})$, where F_{ν_0} is the cumulative distribution functions of a random variable following a t distribution with ν_0 degrees of freedom, which means that the link function is $g = F_{\nu_0}$.

Note that the main effects for non-spatiotemporal covariates have a standard linear regression structure $\mathbf{x}_{i,t}^\top \boldsymbol{\beta}$, with a weakly informative prior for $\boldsymbol{\beta}$ (Gelman et al., 2014, p. 55). Also, the main effects for space covariates have a standard linear regression structure $\mathbf{z}_{i,t}^\top \boldsymbol{\gamma}$, following an improper conditionally autoregressive (CAR) model for $\boldsymbol{\gamma}$ (Banerjee et al., 2014, p. 81). Furthermore, the main effects for time are included in the linear predictor through $\delta_t = \xi t$, with a weakly informative prior for ξ . Lastly, the main effects for spatiotemporal interactions $\theta_{i,t} + \phi_{i,t}$ have two components. On the one hand, $\theta_{i,t}$ captures region-wide heterogeneity (unstructured variation) by means of $\text{N}(0, 1/\tau_t)$, where τ_t is a precision parameter controlling the magnitude of $\theta_{i,t}$. And on the other, $\phi_{i,t}$ captures regional clustering (spatially structured variability) via $\text{CAR}(\lambda_t)$, where λ_t is a precision parameter as before.

CAR models are very convenient computationally, since the method for exploring the posterior distribution is in itself a conditional algorithm, the Gibbs sampler, which also

eliminates the need for matrix inversion. However, CAR models have two main theoretical and computational challenges, namely, model impropriety and precision parameter selection. Banerjee et al. (2014, p. 155) recommend to ignore impropriety and work with the intrinsic CAR specification, since we are using it just as a prior distribution and not to model the data directly. Even though this is the usual approach it requires some care: This improper CAR prior is a pairwise difference prior that is identified only up to an additive constant. Thus, in order to identify an intercept term (say β_1), we must add the constraint $\sum_{i=1}^I \phi_{i,t} = 0$ (this constraint is imposed numerically during computation). Moreover, τ_t and λ_t cannot be chosen arbitrarily large, since $\theta_{i,t}$ and $\phi_{i,t}$ would become unidentifiable. After all, we have only a single $y_{i,t}$ in order to estimate two random effects for each i and each t . To make the prior specification $\tau_t \sim \mathbf{G}(a_\tau, b_\tau)$ and $\lambda_t \sim \mathbf{G}(a_\lambda, b_\lambda)$ sensible, Banerjee et al. (2014, p. 156) recommend a prior specification that leads to

$$\text{SD}(\theta_{i,t}) = \frac{1}{\sqrt{\tau_t}} \approx \frac{1}{0.7\sqrt{\bar{m}}\lambda_t} \approx \text{SD}(\phi_{i,t}), \quad (8)$$

where \bar{m} is the average number of neighbors.

Define $\mathbf{y} = (y_{1,1}, \dots, y_{I,T})$, $\boldsymbol{\omega} = (\omega_{1,1}, \dots, \omega_{I,T})$, $\boldsymbol{\theta} = (\theta_{1,1}, \dots, \theta_{I,T})$, $\boldsymbol{\phi} = (\phi_{1,1}, \dots, \phi_{I,T})$, $\boldsymbol{\kappa} = (\kappa_1, \dots, \kappa_T)$, $\boldsymbol{\tau} = (\tau_1, \dots, \tau_T)$, $\boldsymbol{\lambda} = (\lambda_1, \dots, \lambda_T)$, and also, $\boldsymbol{\Upsilon} = (\boldsymbol{\omega}, \boldsymbol{\theta}, \boldsymbol{\phi}, \boldsymbol{\beta}, \boldsymbol{\gamma}, \boldsymbol{\xi})$. Parameter estimates can be obtained from the posterior distribution

$$p(\boldsymbol{\Upsilon} | \mathbf{y}) \propto p(\mathbf{y} | \boldsymbol{\omega}) p(\boldsymbol{\omega} | \boldsymbol{\theta}, \boldsymbol{\phi}, \boldsymbol{\beta}, \boldsymbol{\gamma}, \boldsymbol{\xi}, \boldsymbol{\kappa}) p(\boldsymbol{\theta} | \boldsymbol{\tau}) p(\boldsymbol{\phi} | \boldsymbol{\lambda}) p(\boldsymbol{\beta}) p(\boldsymbol{\gamma}) p(\boldsymbol{\xi}) p(\boldsymbol{\kappa}) p(\boldsymbol{\tau}) p(\boldsymbol{\lambda}),$$

where according to (6) and (7),

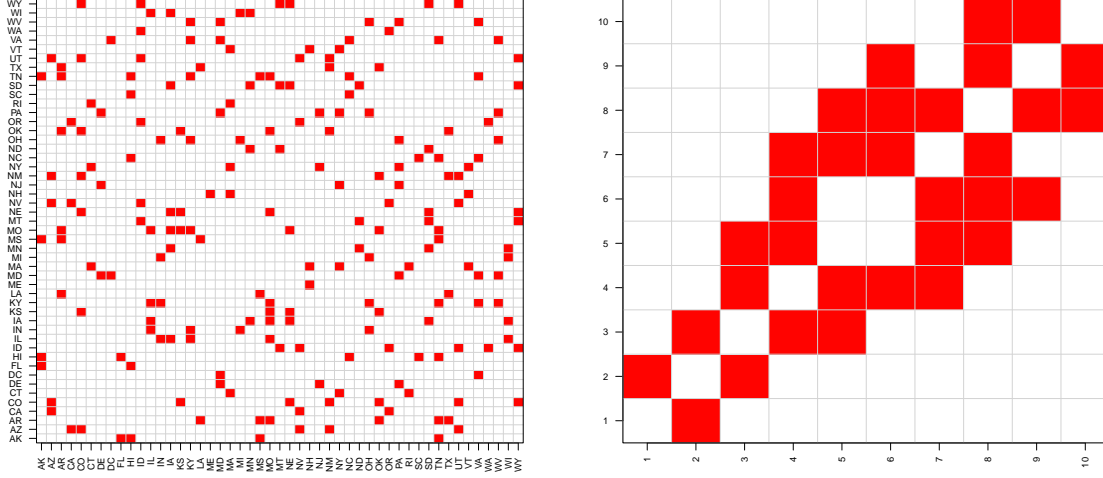
$$\begin{aligned} p(\boldsymbol{\omega} | \boldsymbol{\beta}, \boldsymbol{\gamma}, \boldsymbol{\theta}, \boldsymbol{\xi}, \boldsymbol{\phi}, \boldsymbol{\kappa}) &= \prod_{i=1}^I \prod_{t=1}^T \mathbf{N}(\omega_{i,t} | \mathbf{x}_i^\top \boldsymbol{\beta} + \mathbf{z}_i^\top \boldsymbol{\gamma} + \xi_t + \theta_{i,t} + \phi_{i,t}, 1/\kappa_t), \\ p(\boldsymbol{\theta} | \boldsymbol{\tau}) &= \mathbf{N}_{IT}(\boldsymbol{\theta} | \mathbf{0}, \text{diag}[(1/\tau_1)\mathbf{I}_I, \dots, (1/\tau_T)\mathbf{I}_I]), \\ p(\boldsymbol{\phi} | \boldsymbol{\lambda}) &= \text{CAR}(\boldsymbol{\phi} | \text{diag}[\lambda_1 \mathbf{W}, \dots, \lambda_T \mathbf{W}]), \end{aligned}$$

$$p(\boldsymbol{\beta}) p(\boldsymbol{\gamma}) p(\boldsymbol{\xi}) p(\boldsymbol{\kappa}) p(\boldsymbol{\tau}) p(\boldsymbol{\lambda}) = p(\boldsymbol{\xi}) \times \prod_{k=1}^K p(\beta_k) \times \prod_{\ell=1}^L p(\gamma_\ell) \times \prod_{t=1}^T p(\kappa_t) p(\tau_t) p(\lambda_t),$$

with $p(\boldsymbol{\xi})$, $p(\beta_k)$, $p(\gamma_\ell)$, $p(\kappa_t)$, $p(\tau_t)$, $p(\lambda_t)$ specified as in (7), and $\mathbf{W} = [W_{i,j}]$ is a square matrix of size $I \times I$ such that

$$W_{i,j} = \begin{cases} m_i, & i = j; \\ -1, & i \sim j; \\ 0, & \text{otherwise,} \end{cases}$$

where m_i is the number of neighbors of \mathbf{s}_i (see Figure 5), and $i \sim j$ means that units i and j are neighbors. Full conditional distributions are derived looking at the dependencies



(a) States neighbor matrix

(b) Regions neighbor matrix

Figure 5: States and regions neighbors used to specify precision matrices. Red boxes denote neighbor elements.

in $p(\mathbf{Y} | \mathbf{y})$. Let $\mathbf{Y}^{(b)}$ be the vector of model parameters at iteration b of the algorithm, for $b = 1, \dots, B$. Given a starting point $\mathbf{Y}^{(0)}$, we consider a Gibbs sampler (with a step with a numerical constraint) updating $\mathbf{Y}^{(b-1)}$ to $\mathbf{Y}^{(b)}$ until convergence as follows:

1. Sample

$$\omega_{i,t} | \text{rest} \sim \begin{cases} \text{TN}_{(-\infty, 0]}(\mathbf{x}_i^\top \boldsymbol{\beta} + \mathbf{z}_i^\top \boldsymbol{\gamma} + \xi t + \theta_{i,t} + \phi_{i,t}, 1/\kappa_t), & y_{it} = 0; \\ \text{TN}_{(0, +\infty)}(\mathbf{x}_i^\top \boldsymbol{\beta} + \mathbf{z}_i^\top \boldsymbol{\gamma} + \xi t + \theta_{i,t} + \phi_{i,t}, 1/\kappa_t), & y_{it} = 1, \end{cases}$$

for $i = 1, \dots, I$, $t = 1, \dots, T$.

2. Sample

$$\boldsymbol{\beta} | \text{rest} \sim N_K(\mathbf{V}_\beta [\mathbf{X}^\top \boldsymbol{\Sigma}_\omega^{-1}(\mathbf{w} - \mathbf{Z}\boldsymbol{\gamma} - \mathbf{t}\xi - \boldsymbol{\theta} - \boldsymbol{\phi})], \mathbf{V}_\beta)$$

where $\mathbf{V}_\beta = (\sigma_0^{-2} \mathbf{I}_K + \mathbf{X}^\top \boldsymbol{\Sigma}_\omega^{-1} \mathbf{X})^{-1}$, $\boldsymbol{\Sigma}_\omega^{-1} = \text{diag}[\mathbf{1}_I \otimes \boldsymbol{\kappa}]$, $\mathbf{t} = \mathbf{1}_I \otimes [t_1, \dots, t_T]^\top$, $\mathbf{X} = [\mathbf{X}_1^\top, \dots, \mathbf{X}_I^\top]^\top$, with $\mathbf{X}_i = \mathbf{1}_T \otimes \mathbf{x}_i^\top$ for $i = 1, \dots, I$, $\mathbf{Z} = [\mathbf{Z}_1^\top, \dots, \mathbf{Z}_I^\top]^\top$, with $\mathbf{Z}_i = \mathbf{1}_T \otimes \mathbf{z}_i^\top$ for $i = 1, \dots, I$.

3. Sample

$$\boldsymbol{\gamma} | \text{rest} \sim N_L(\mathbf{V}_\gamma [\mathbf{Z}^\top \boldsymbol{\Sigma}_\omega^{-1}(\mathbf{w} - \mathbf{X}\boldsymbol{\beta} - \mathbf{t}\xi - \boldsymbol{\theta} - \boldsymbol{\phi})], \mathbf{V}_\gamma)$$

where $\mathbf{V}_\gamma = (\sigma_0^{-2} \mathbf{W}^* + \mathbf{Z}^\top \boldsymbol{\Sigma}_\omega^{-1} \mathbf{Z})^{-1}$ and \mathbf{W}^* is a precision matrix of size $L \times L$ defined accordingly (see Figure 5).

4. Sample

$$\xi \mid \text{rest} \sim \text{N} (V_\xi [\mathbf{t}^\top \boldsymbol{\Sigma}_\omega^{-1} (\mathbf{w} - \mathbf{X}\boldsymbol{\beta} - \mathbf{Z}\boldsymbol{\gamma} - \boldsymbol{\theta} - \boldsymbol{\phi})], V_\xi)$$

where $V_\xi = (\sigma_0^{-2} + \mathbf{t}^\top \boldsymbol{\Sigma}_\omega^{-1} \mathbf{t})^{-1}$.

5. Sample

$$\boldsymbol{\theta}_t \mid \text{rest} \sim \text{N}_I (\mathbf{V}_t [\kappa_t (\boldsymbol{\omega}_t - \mathbf{X}_t \boldsymbol{\beta} - \mathbf{Z}_t \boldsymbol{\gamma} - \mathbf{t}_t \xi - \boldsymbol{\phi}_t)], \mathbf{V}_t)$$

where $\boldsymbol{\theta}_t = (\theta_{1t}, \dots, \theta_{It})$, $\mathbf{V}_t = (\tau_t + \kappa_t)^{-1} \mathbf{I}_I$, $\boldsymbol{\omega}_t = (\omega_{1t}, \dots, \omega_{It})$, $\mathbf{X}_t = [\mathbf{x}_1, \dots, \mathbf{x}_I]^\top$, $\mathbf{Z}_t = [\mathbf{z}_1, \dots, \mathbf{z}_I]^\top$, and $\mathbf{t}_t = t \mathbf{1}_I$, for $t = 1, \dots, T$.

6. Sample

$$\boldsymbol{\phi}_t \mid \text{rest} \sim \text{N}_I (\mathbf{V}_t [\kappa_t (\boldsymbol{\omega}_t - \mathbf{X}_t \boldsymbol{\beta} - \mathbf{Z}_t \boldsymbol{\gamma} - \mathbf{t}_t \xi - \boldsymbol{\theta}_t)], \mathbf{V}_t)$$

where $\boldsymbol{\phi}_t = (\phi_{1t}, \dots, \phi_{It})$ and $\mathbf{V}_t = (\lambda_t \mathbf{W} + \kappa_t \mathbf{I}_I)^{-1}$, for $t = 1, \dots, T$.

7. Center $\boldsymbol{\phi}_t$ around its own mean in order to impose the constrain $\sum_{i=1}^I \phi_{i,t} = 0$, for $t = 1, \dots, T$.

8. Sample $\kappa_t \mid \text{rest} \sim \text{G}((\nu_0 + I)/2, (\nu_0 + \|\boldsymbol{\omega}_t - \mathbf{X}_t \boldsymbol{\beta} - \mathbf{Z}_t \boldsymbol{\gamma} - \mathbf{t}_t \xi - \boldsymbol{\theta}_t - \boldsymbol{\phi}_t\|^2)/2)$, for $t = 1, \dots, T$.

9. Sample $\tau_t \mid \text{rest} \sim \text{G}(a_\tau + \frac{I}{2}, b_\tau + \frac{1}{2} \|\boldsymbol{\theta}_t\|^2)$, for $t = 1, \dots, T$.

10. Sample $\lambda_t \mid \text{rest} \sim \text{G}(a_\lambda + \frac{1}{2} \text{rank}(\mathbf{W}), b_\lambda + \frac{1}{2} \boldsymbol{\phi}_t^\top \mathbf{W} \boldsymbol{\phi}_t)$, for $t = 1, \dots, T$.

Now, we implement the model by considering the Google flu data corresponding to the first 12 weeks of 2013. Outbreaks of influenza are commonly observed during weeks 1 to 8 (Winter season). The proportion of states with Google flue index greater than 7500 cases goes down straight to zero after week 8. Then, we have an align dataset with $I = 49$ states (subjects) and $T = 12$ weeks (period times) that lead to 637 observations possibly correlated in time and space. Thus, we consider the linear predictor given by

$$F_{\nu_0}^{-1}(\pi_{i,t}) = \beta_1 + \beta_2 x_{i,1} + \beta_3 x_{i,2} + \gamma_\ell z_{i,\ell} + \xi t + \theta_{i,t} + \phi_{i,t} \quad (9)$$

where $x_{i,1}$ and $x_{i,2}$ are the proportion of white population and the proportion of population over 65 years old, respectively, for state i in 2013, according to Kaiser Family Foundation (<http://kff.org/>), and $z_{i,\ell}$ is an indicator variable pointing out if state i belongs to region ℓ or not, according to according to the U.S. Department of Health and Human Services (HHS, <http://www.hhs.gov/iea/regional/>; see Figure 6). Therefore, β_1 is the mean global effect, β_k is the fixed effect of covariate k , for $k = 2, 3$, γ_ℓ is the fixed spacial effect of region ℓ , for $\ell = 1, \dots, 10$, ξ is the fixed effect of time, and $\phi_{i,t} + \theta_{i,t}$ is the random spatiotemporal effect considering heterogeneity and clustering.

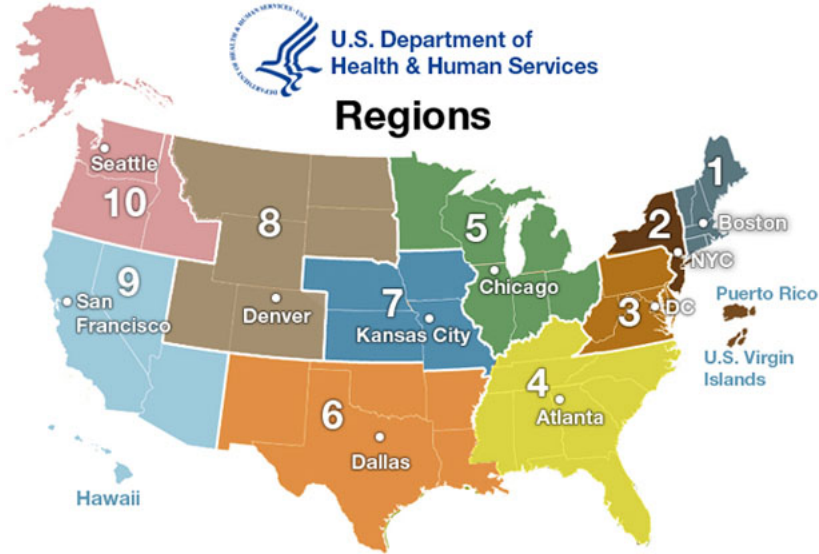


Figure 6: Regional offices according to the U.S. Department of Health and Human Services..

We implement the MCMC algorithm given above drawing $B = 25000$ samples from the posterior distribution $p(\Upsilon \mid \mathbf{y})$ after thinning the original chain every 10 observations and a burn-in period of 5000 iterations. To do so, we weakly concentrate the prior distribution of β_k , γ_ℓ , and ξ around 0, and that of κ_t , τ_t , and λ_t around 1, by following the prior specification given in (8) with $\sigma_0^2 = 100$, $\nu_0 = a_\tau = b_\tau = a_\lambda = 2$, and $b_\lambda = (0.7^2)\bar{m}b_\tau$. Notice that ν_0 is set equal to 2 because a t_2 distribution has an infinite variance. Trace and autocorrelation plots of the regression parameters show that the corresponding chains achieve convergence quickly. However, in some particular cases, there are signs of serious autocorrelation (in order to address this issue we thin the chain as specified).

Figure 7 summarizes the posterior distribution of β , ξ , and γ . The proportion of the white population have a positive significant impact on the response, which leads to an increment in the probability that the state is above the threshold, whereas the global mean and the proportion of population over 65 do not. Even though most deaths associated with influenza in industrialized countries occur among the elderly over 65 years of age, this covariate results not significant because it has little variation across the states ($CV \doteq 11\%$) and the proportion of population over 65 in each state is just a small fraction of the whole state population (be aware of the “ecological fallacy”). Furthermore, all the regions delimited by the HHS have a significant impact on the response, excepting regions 6 and 9 (see Figure 6). This finding is reasonable since these regions are neighbors and are the smallest regions in terms of extension and population.

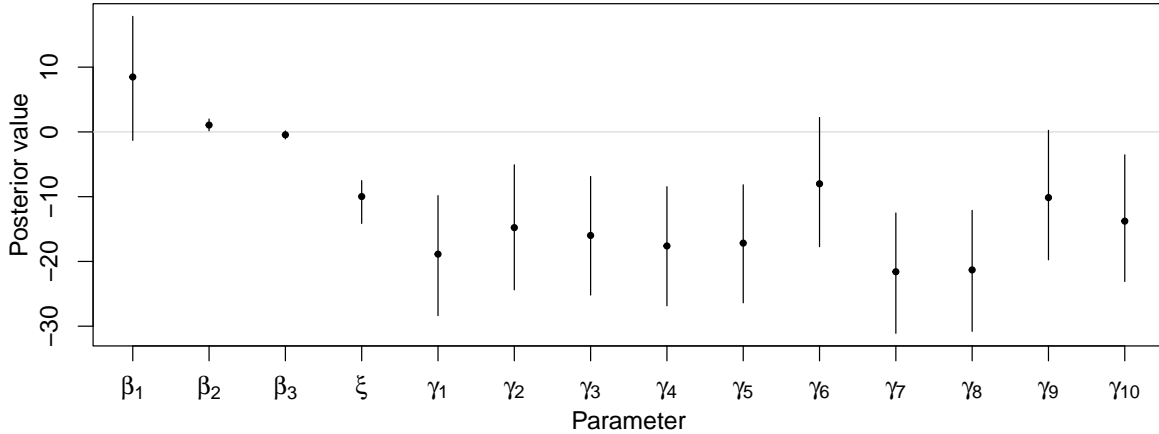


Figure 7: Posterior mean and 95% quantile-based credible intervals for β , ξ , and γ .

In addition, it is not surprising that in general regions have a negative influence on the response since these regions independently address needs of communities and individuals through HHS programs and policies. Finally, the effect of time is also significant since it is a well known that outbreaks of flue are highly correlated with seasons and we consider a time transition frame.

On the other hand, Figure 8 displays the posterior mean for the sum of the heterogeneity and clustering random effects $\theta_{i,t} + \phi_{i,t}$. As expected, these effects clearly go down toward 0 after week 8 due to the seasonal behavior of the response. Even though all the states reveal similar patterns, the model is also useful to identify subject-specific dynamic effects. For instance, consider the case of Maine (ME), which is the state with the highest proportion of white population in 2013.

5 Species sampling modeling

We consider the species sampling model (SSS)

$$p(X_{n+1} \in B \mid X_1, \dots, X_n) = \sum_{k=1}^{K^n} q_k^n(\mathbf{m}^n) \delta_{\tilde{X}_k}(B) + q_{K^n+1}^n(\mathbf{m}^n) G_0(B)$$

where G_0 is a non-atomic measure (Rodríguez and Quintana, 2015). First of all, in order to understand and develop the MCMC algorithms presented below, we find an expression for $E(K^n)$, the expected value of the number of distinct species among X_1, \dots, X_n .

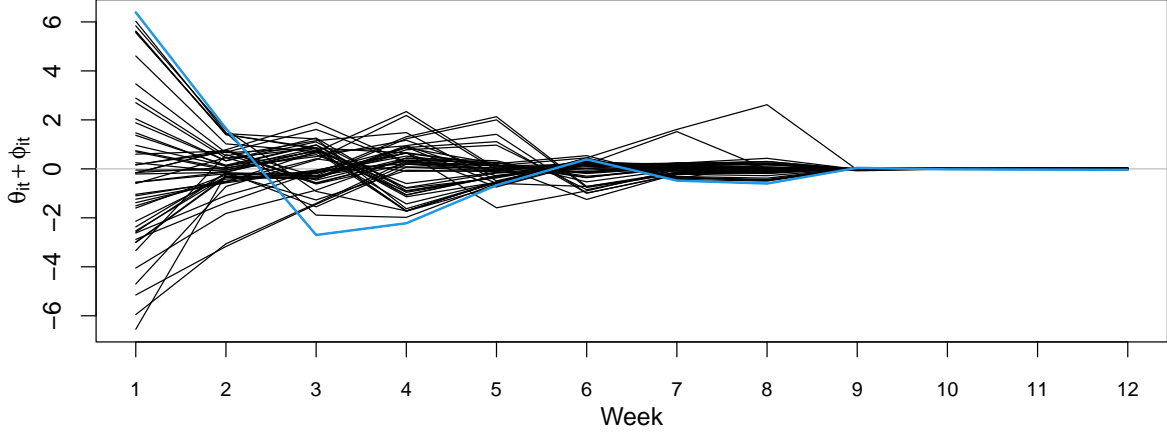


Figure 8: Posterior mean for the dynamic random effects $\theta_{i,t} + \phi_{i,t}$. The blue line corresponds to Maine, which is the state with the highest proportion of white population in 2013.

Let W_1, \dots, W_n be a sequence of binary random variables such that

$$W_i := \begin{cases} 1, & X_i \text{ corresponds to a species that has not been observed in } X_1, \dots, X_{i-1}; \\ 0, & \text{otherwise,} \end{cases}$$

for $i = 1, \dots, n$. Since the first observation is necessarily a new observation we have that $W_1 \equiv 1$ and

$$\mathbb{E}(K^n) = \mathbb{E}\left(\sum_{i=1}^n W_i\right) = \sum_{i=1}^n \mathbb{E}(W_i) = 1 + \sum_{i=2}^n \mathbb{E}(W_i).$$

Let \mathcal{M}_k denote the set of all vectors of length k with positive, integer entries that add up to n , i.e., $\mathcal{M}_k := \{(m_1, \dots, m_k) \in \mathbb{N}^k : m_1 + \dots + m_k = n\}$. Case by case, we see that

$$\begin{aligned} \mathbb{E}(W_2) &= \sum_{\mathcal{M}_1} p(m_1^1, 1) \\ \mathbb{E}(W_3) &= \sum_{\mathcal{M}_1} p(m_1^2, 1) + \sum_{\mathcal{M}_2} p(m_1^2, m_2^2, 1) \\ \mathbb{E}(W_4) &= \sum_{\mathcal{M}_1} p(m_1^3, 1) + \sum_{\mathcal{M}_2} p(m_1^3, m_2^3, 1) + \sum_{\mathcal{M}_3} p(m_1^3, m_2^3, m_3^3, 1) \\ &\vdots \\ \mathbb{E}(W_i) &= \sum_{\mathcal{M}_1} p(m_1^{i-1}, 1) + \sum_{\mathcal{M}_2} p(m_1^{i-1}, m_2^{i-1}, 1) + \dots + \sum_{\mathcal{M}_{i-1}} p(m_1^{i-1}, \dots, m_{i-1}^{i-1}, 1) \end{aligned}$$

and therefore

$$\mathbb{E}(W_i) = \sum_{k=1}^{i-1} \sum_{\mathcal{M}_k} p(m_1^{i-1}, \dots, m_k^{i-1}, 1).$$

Recalling the following fact given in Pitman (1995, p. 152),

$$p(m_1^{i-1}, \dots, m_k^{i-1}, 1) = p(m_1^{i-1}, \dots, m_k^{i-1}) q_{k+1}^{i-1}(m_1^{i-1}, \dots, m_k^{i-1}), \quad i = 2, \dots, n,$$

we finally get that the expected value of the number of distinct species is given by

$$\mathbb{E}(K^n) = 1 + \sum_{i=2}^n \sum_{k=1}^{i-1} \sum_{\mathcal{M}_k} p(m_1^{i-1}, \dots, m_k^{i-1}) q_{k+1}^{i-1}(m_1^{i-1}, \dots, m_k^{i-1}).$$

In order to verify this result, we consider two particular scenarios, namely, the Chinese restaurant process (CRP) and the Pitman-Yor process (PYP):

CRP In this case, the predictive probability function (PPF) is given by $q_{k+1}^{i-1}(m_1^{i-1}, \dots, m_k^{i-1}) = \frac{\theta}{\theta+i-1}$ (Müller and Rodriguez, 2013, p. 83), and therefore

$$\mathbb{E}(K^n) = 1 + \sum_{i=2}^n \frac{\theta}{\theta+i-1} \sum_{k=1}^{i-1} \sum_{\mathcal{M}_k} p(m_1^{i-1}, \dots, m_k^{i-1}) = 1 + \sum_{i=2}^n \frac{\theta}{\theta+i-1}$$

since

$$\sum_{k=1}^{i-1} \sum_{\mathcal{M}_k} p(m_1^{i-1}, \dots, m_k^{i-1}) = 1, \quad i = 1, \dots, n,$$

which leads to

$$\mathbb{E}(K^n) = \sum_{i=1}^n \frac{\theta}{\theta+i-1}$$

This expression is the same one given in Rodríguez and Quintana (2015, p. 6).

PYP In this case the PPF is given by $q_{k+1}^{i-1}(m_1^{i-1}, \dots, m_k^{i-1}) = \frac{\theta+\sigma k}{\theta+i-1}$ (Müller and Rodriguez, 2013, p. 85), which means that

$$\begin{aligned} \mathbb{E}(K^n) &= 1 + \sum_{i=2}^n \sum_{k=1}^{i-1} \sum_{\mathcal{M}_k} p(m_1^{i-1}, \dots, m_k^{i-1}) \frac{\theta + \sigma k}{\theta + i - 1} \\ &= 1 + \sum_{i=2}^n \frac{\theta}{\theta + i - 1} \sum_{k=1}^{i-1} \sum_{\mathcal{M}_k} p(m_1^{i-1}, \dots, m_k^{i-1}) \\ &\quad + \sum_{i=2}^n \frac{\sigma}{\theta + i - 1} \sum_{k=1}^{i-1} \sum_{\mathcal{M}_k} k p(m_1^{i-1}, \dots, m_k^{i-1}) \end{aligned}$$

and therefore

$$\mathbb{E}(K^n) = \sum_{i=1}^n \frac{\theta}{\theta + i - 1} + \sum_{i=2}^n \frac{\sigma}{\theta + i - 1} \zeta_i$$

with

$$\zeta_i := \sum_{k=1}^{i-1} \sum_{\mathcal{M}_k} k p(m_1^{i-1}, \dots, m_k^{i-1}), \quad i = 2, \dots, n.$$

Now, consider the stick breaking prior of the form $G = \sum_{l=1}^{\infty} \omega_l \delta_{X_l^*}$ where $X_l^* \stackrel{\text{iid}}{\sim} G_0$, $\omega_l = z_l \prod_{k<l} (1 - z_k)$, and $z_l \stackrel{\text{iid}}{\sim} H^\theta$ for all $l = 1, 2, \dots$, with H^θ a probability distribution on $[0, 1]$ indexed by the vector of parameters θ . In what follows we show that the exchangeable partition probability function (EPPF) induced by this stick breaking prior is given by

$$p(m_1^n, \dots, m_{K^n}^n | \theta) = \sum_{\sigma \in \mathcal{P}_{K^n}} \left[\prod_{k=1}^{K^n} \frac{\gamma_\theta \left(m_{\sigma_k}^n, \sum_{j=k+1}^{K^n} m_{\sigma_j}^n \right)}{1 - \gamma_\theta \left(0, \sum_{j=k}^{K^n} m_{\sigma_j}^n \right)} \right] \quad (10)$$

where \mathcal{P}_{K^n} denotes the set of all permutations of $\{1, \dots, K^n\}$, $\sigma = (\sigma_1, \dots, \sigma_{K^n})$, and $\gamma_\theta(x, y) = \mathbb{E}(z^x (1 - z)^y)$ with $z \sim H^\theta$.

If X_1, \dots, X_n is a iid sample from G , then this sequence is exchangeable and there exists a positive probability of ties among the X_i s. Furthermore, the EPPF associated with this prior is given by

$$p(\mathbf{m}^n | \theta) = \sum_{(j_1, \dots, j_{K^n}) \in \mathcal{J}_{K^n}} \mathbb{E} \left(\prod_{k=1}^{K^n} \omega_{j_k}^{m_k^n} \right) \quad (11)$$

where $\mathbf{m} = (m_1^n, \dots, m_{K^n}^n)$ and \mathcal{J}_{K^n} is the set of all possible sequences of distinct positive integers of length K^n (Pitman, 1996, p. 256). Then, by expanding the summation, the previous expression becomes

$$p(\mathbf{m}^n | \theta) = \sum_{j_1} \sum_{j_2 \notin \{j_1\}} \sum_{j_3 \notin \{j_1, j_2\}} \dots \sum_{j_{K^n} \notin \{j_1, \dots, j_{K^n-1}\}} \mathbb{E} \left(\prod_{k=1}^{K^n} \left(z_{j_k} \prod_{h < j_k} (1 - z_h) \right)^{m_k^n} \right).$$

First, we consider the scenario in which $j_1 < j_2 < \dots < j_{K^n}$. Therefore,

$$\begin{aligned} \prod_{k=1}^{K^n} \left(z_{j_k} \prod_{h < j_k} (1 - z_h) \right)^{m_k^n} &= \prod_{k=1}^{K^n} z_{j_k}^{m_k^n} (1 - z_1)^{m_k^n} (1 - z_2)^{m_k^n} \dots (1 - z_{j_k-1})^{m_k^n} \\ &= [z_{j_1} \dots z_{K^n}]^{S_1^n} \cdot [(1 - z_1) \dots (1 - z_{j_1-1})]^{S_1^n} \cdot [(1 - z_{j_1}) \dots (1 - z_{j_2-1})]^{S_2^n} \\ &\quad \cdot [(1 - z_{j_2}) \dots (1 - z_{j_3-1})]^{S_3^n} \dots \cdot [(1 - z_{j_{(K^n-1)}}) \dots (1 - z_{j_{(K^n)}-1})]^{S_{K^n}^n} \end{aligned}$$

where $S_k^n = \sum_{j=k}^{K^n} m_j^n$ for $k = 1, \dots, K^n$.

Associating terms and recalling the fact that $z_l \stackrel{\text{iid}}{\sim} H^\theta$ for $l = 1, 2, \dots$ we get that

$$\mathbb{E} \left(\prod_{k=1}^{K^n} \omega_{j_k}^{m_k^n} \right) = \prod_{k=1}^{K^n} \mathbb{E} \left(z^{m_k} (1-z)^{S_{k+1}^n} \right) \left(\mathbb{E} \left((1-z)^{S_k} \right) \right)^{d_k}$$

where $z \sim H^\theta$ and $d_k = j_k - j_{k-1} - 1$ for $k = 1, \dots, K^n$, which represent the sizes of the ‘‘gaps’’ between the labels of two consecutive observed species, with the convention $j_0 = 0$ (Rodríguez and Quintana, 2015, p. 14).

Now, recognizing the symmetry of the summation in (11) and all the possible ‘‘gaps’’ we obtain that

$$\begin{aligned} p(\mathbf{m}^n | \boldsymbol{\theta}) &= \sum_{d_1=0}^{\infty} \dots \sum_{d_{K^n}=0}^{\infty} \mathbb{E} \left(\prod_{k=1}^{K^n} \omega_{j_k}^{m_k^n} \right) \\ &= \prod_{k=1}^{K^n} \left\{ \mathbb{E} \left(z^{m_k} (1-z)^{S_{k+1}^n} \right) \sum_{d_k=0}^{\infty} \left(\mathbb{E} \left((1-z)^{S_k} \right) \right)^{d_k} \right\} \end{aligned}$$

Since the last summation is a geometric series then we finally get that

$$p(\mathbf{m}^n | \boldsymbol{\theta}) = \prod_{k=1}^{K^n} \frac{\mathbb{E} \left(z^{m_k} (1-z)^{S_{k+1}^n} \right)}{1 - \mathbb{E} \left((1-z)^{S_k} \right)}$$

which precisely corresponds to the expression given in (11).

We consider the data discussed in Lijoi et al. (2007, Sec. 4.2). The basic sample consists of $n = 2586$ expressed sequence tags and this gives $K^n = 1825$ different CDNA fragments each of which represents a unique gene. If r_i denotes the number of clusters of size i , then the dataset gives $r_i = 1434, 253, 71, 33, 11, 6, 2, 3, 1, 2, 2, 1, 1, 1, 2, 1, 1$ with $i \in \{1, 2, \dots, 14\} \cup \{16, 23, 27\}$. This means we are observing 1434 clusters of size 1, 253 clusters of size 2, and so on.

Here, we develop MCMC algorithms for performing Bayesian estimation of the parameters of a CRP and a PYP using this dataset. These algorithms were designed according to the posterior distribution

$$p(\boldsymbol{\theta} | \mathbf{m}^n) \propto p(\mathbf{m}^n | \boldsymbol{\theta}) p(\boldsymbol{\theta})$$

where $\boldsymbol{\theta}$ is the vector of parameters of the process and $\mathbf{m}^n = (m_1^n, \dots, m_{K^n}^n)$. Below we describe the algorithms for performing Bayesian estimation of $\boldsymbol{\theta}$. Let $\boldsymbol{\theta}^{(m)}$ denote the parameter vector at iteration m of the algorithm, $m = 0, 1, \dots, M$. Given a starting point of the parameter $\boldsymbol{\theta}^{(0)}$, we run the sampler updating $\boldsymbol{\theta}^{(m-1)}$ to $\boldsymbol{\theta}^{(m)}$ until convergence according to the corresponding description.

CRP Here $\theta = \theta$ and

$$p(\theta|\mathbf{m}^n) \propto \left[\theta^{K^n} \frac{\Gamma(\theta)}{\Gamma(\theta + n)} \prod_{j=1}^{K^n} \Gamma(m_j^n) \right] \times \mathbf{G}(\theta|a_\theta, b_\theta).$$

The MCMC algorithm is as follows:

1. Compute $\eta^{(m-1)} = \log \theta^{(m-1)}$.
2. Sample $\eta^* \sim \mathbf{N}(\eta^{(m-1)}, b_\eta)$, where b_η is a tuning parameter.
3. Compute $r = p_\eta(\eta^*|\mathbf{m}^n)/p_\eta(\eta^{(m-1)}|\mathbf{m}^n)$ where $p_\eta(\eta|\mathbf{m}^n) = p(e^\eta|\mathbf{m}^n) \times e^\eta$.
4. Set

$$\eta^{(m)} = \begin{cases} \eta^*, & \text{with probability } r; \\ \eta^{(m-1)}, & \text{with probability } 1 - r. \end{cases}$$

5. Compute $\theta^{(m)} = \exp \{ \eta^{(m)} \}$.
6. Repeat until convergence.

Notice that in the Metropolis step above we do the transformation $\eta = \log(\theta)$ to consider the range of θ in the random-walk proposal. The corresponding Jacobian (e^η) is taken into account in the computations through $p_\eta(\eta|\mathbf{m}^n)$.

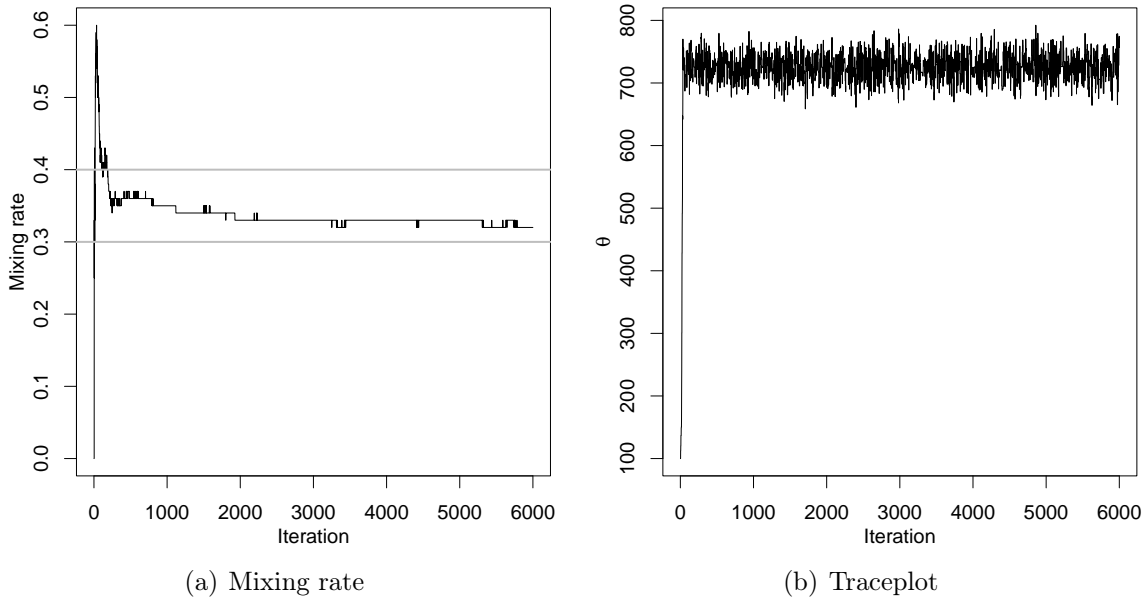


Figure 9: Mixing rates associated with the Metropolis algorithm and traceplot for θ in the CRP.

We run the sampler with $M = 6000$ iterations using as hyperparameters $a_\theta = 1$ and $b_\theta = 1$, and $b = 0.1$ as tuning parameter (which leads to nice mixing rates between 30% and 40%, see left panel of Figure 9). In addition, we use a burn-in period with 1000 iterations and, in order to have approximately independent draws, select one sample from each 50 iterations. As a consequence a total of 100 samples are selected altogether (the chain quickly achieves convergence, see right panel of Figure 9). Those 100 samples are approximately independent and identically distributed according to the corresponding posterior distribution and form the basis of posterior inference. Finally, table 4 summarizes the posterior distribution of θ .

Parameter	Mean	Median	SD	Q 2.5%	Q 97.5%
θ	723.42	724.04	22.13	679.90	768.25

Table 4: Posterior summaries for θ in the CRP.

PYP Here $\boldsymbol{\theta} = (\theta, \sigma)$ and

$$p(\boldsymbol{\theta}|\mathbf{m}^n) \propto \left[\frac{\Gamma(\theta + 1)}{\Gamma(\theta + K^n \sigma) \Gamma(\theta + n)} \prod_{j=1}^{K^n} (\theta + j\sigma) \frac{\Gamma(m_j^n - \sigma)}{\Gamma(1 - \sigma)} \right] \\ \times \text{NT}_{(-\sigma, \infty)}(\theta|a_\theta, b_\theta) \times \text{Be}(\sigma|a_\sigma, b_\sigma)$$

The MCMC algorithm is as follows:

1. Update $\sigma^{(m-1)}$ given $\theta^{(m-1)}$ and \mathbf{m}^n as follows:
 - i. Compute $\eta^{(m-1)} = \text{logit } \sigma^{(m-1)}$, with $\text{logit } x = \log \frac{x}{1-x}$.
 - ii. Sample $\eta^* \sim N(\eta^{(m-1)}, b_\eta)$, where b_η is a fixed positive constant.
 - iii. Compute $r = p_\eta(\eta^*|\theta^{(m-1)}, \mathbf{m}^n) / p_\eta(\eta^{(m-1)}|\theta^{(m-1)}, \mathbf{m}^n)$ where

$$p_\eta(\eta|\theta, \mathbf{m}^n) = p(\text{logit}^{-1} \eta|\theta, \mathbf{m}^n) \times \frac{e^\eta}{(e^\eta + 1)^2}$$

$$\text{with } \text{logit}^{-1} x = \frac{e^x}{e^x + 1}.$$

- iv. Set

$$\eta^{(m)} = \begin{cases} \eta^*, & \text{with probability } r; \\ \eta^{(m-1)}, & \text{with probability } 1 - r. \end{cases}$$

- v. Compute $\sigma^{(m)} = \text{logit}^{-1} \eta^{(m)}$.

2. Update $\theta^{(m-1)}$ given $\sigma^{(m)}$ and \mathbf{m}^n as follows:

- i. Compute $\psi^{(m-1)} = \log(\theta^{(m-1)} + \sigma^{(m)})$.
- ii. Sample $\psi^* \sim N(\psi^{(m-1)}, b_\psi)$, where b_ψ is a fixed positive constant.
- iii. Compute $s = p_\psi(\psi^* | \sigma^{(m)}, \mathbf{m}^n) / p_\psi(\psi^{(m-1)} | \sigma^{(m)}, \mathbf{m}^n)$, where

$$p_\psi(\psi | \theta, \mathbf{m}^n) = p(e^\psi - \sigma | \theta, \mathbf{m}^n) \times e^\psi.$$

- iv. Set

$$\psi^{(m)} = \begin{cases} \psi^*, & \text{with probability } s; \\ \psi^{(m-1)}, & \text{with probability } 1 - s. \end{cases}$$

- v. Compute $\theta^{(m)} = \exp\{\psi^{(m)}\} - \sigma^{(m)}$.

- 3. Repeat until convergence.

Notice that in the Metropolis steps above we do two transformations to consider the range of parameters in the random-walk proposals. The corresponding Jacobians are taken into account in the computations.

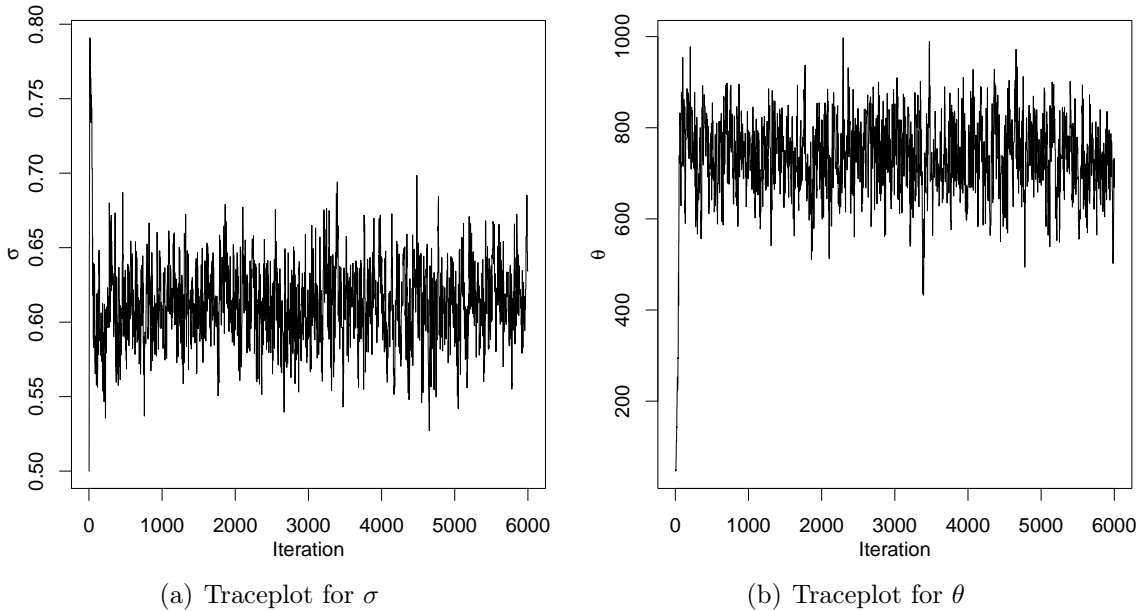


Figure 10: Traceplots for the σ and θ in the PYP.

Once again we run the sampler with $M = 6000$ iterations using as hyperparameters $a_\sigma = 1$, $b_\sigma = 1$, $a_\theta = 723$ and $b_\theta = 100$ (fairly uninformative prior distributions), and $b_\eta = 0.2$ and $b_\psi = .2$ as tuning parameters (which leads to nice mixing rates between 30% and 40% not shown here). Again, we use a burn-in period with 1000 iterations and select one sample from each 50 iterations giving as a result a total

of 100 samples altogether (the chains quickly achieve convergence, see Figure 10). Finally, table 5 summarizes the posterior distribution of σ and θ . These values are certainly close to the corresponding frequentist estimates ($\hat{\sigma}_{\text{mle}} = 0.612$ and $\hat{\theta}_{\text{mle}} = 741$) (Lijoi et al., 2007, p. 778).

Par.	Mean	Median	Sd	Q 2.5%	Q 97.5%
σ	0.61	0.61	0.03	0.56	0.66
θ	733.01	739.00	89.79	569.37	876.31

Table 5: Posterior summaries for σ and θ in the PYP.

Now we extend the previous algorithms to produce predictions on the number of new species in a new sample of size n^* . We consider two extensions: one using purely simulations from the SSM, and other one using the formulas discussed in Lijoi et al. (2007). First of all, recall that

$$p(m_1^n, \dots, m_k^n + 1, \dots, m_{K^n}^n | \boldsymbol{\theta}) = p(\mathbf{m}^n | \boldsymbol{\theta}) q_k^n(\mathbf{m}^n | \boldsymbol{\theta}), \quad k \leq K^n, \quad (12)$$

and

$$p(m_1^n, \dots, m_{K^n}^n, 1 | \boldsymbol{\theta}) = p(\mathbf{m}^n | \boldsymbol{\theta}) q_{K^n+1}^n(\mathbf{m}^n | \boldsymbol{\theta}) \quad (13)$$

where $p(\mathbf{m}^n)$ is the EPPF, $q_k^n(\mathbf{m}^n)$, $k = 1, \dots, K^n + 1$, is the corresponding PPF, and $\mathbf{m}^n = (m_1^n, \dots, m_{K^n}^n)$. Thus, we apply the following algorithm based on direct simulation from the SSM in order to produce predictions on the number of new species:

1. For each $s = 1, \dots, n^*$:
 - i. Compute the distribution given by (12) and (13) for $k = 0, 1, \dots, K^s + 1$.
 - ii. Sample k^* from $\{0, 1, \dots, K^s + 1\}$ according to the previous distribution.
 - iii. Update

$$\mathbf{m}^{s+1} = \begin{cases} \mathbf{m}^s, & \text{if } 1 \leq k^* \leq K^s; \\ (\mathbf{m}^s, 1), & \text{if } k^* = K^s + 1, \end{cases}$$

and

$$K^{s+1} = \begin{cases} K^s, & \text{if } 1 \leq k^* \leq K^s; \\ K^s + 1, & \text{if } k^* = K^s + 1. \end{cases}$$

2. Set $K^{(m)} = K^{n^*+1}$.
3. Repeat for every $\boldsymbol{\theta}^{(m)}$ in the chain for $m = 1, \dots, M$.

On the other hand, considering the formulas to estimating the probability of discovering a new species given in Lijoi et al. (2007, Sec. 3), we implement the following algorithm to produce predictions on the number of new species:

1. Compute the distribution $\Pr(K_{n^*} = k | \theta, \mathbf{m}^n)$ for $k = 0, 1, \dots, n^*$, where $K_{n^*} := K^{n+n^*} - K^n$ is the number of new species in the second (hypothetic) sample of size n^* , by using to the specific formulas given in Lijoi et al. (2007, Sec. 3).
2. Sample k^* from $\{0, 1, \dots, K^s + 1\}$ according to the previous distribution.
3. Set $K^{(m)} = k^*$.
4. Repeat for every $\theta^{(m)}$ in the chain for $m = 1, \dots, M$.

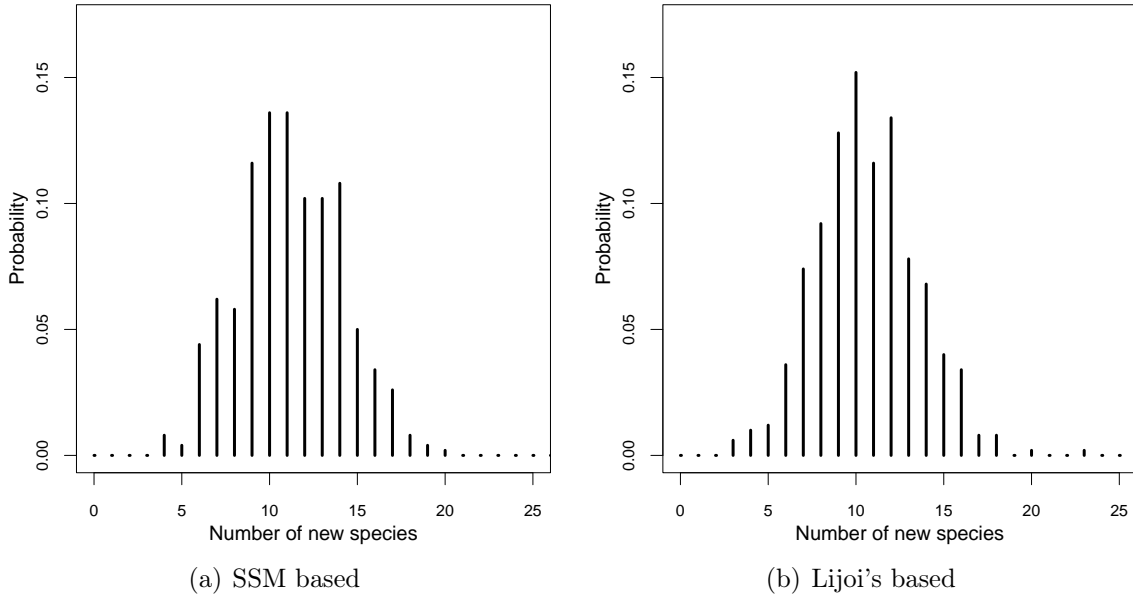


Figure 11: Posterior distribution of the number of new species in a new sample of 100 individuals using purely simulations from the SSM and the formulas discussed in Lijoi et al. (2007).

Once we implement these algorithms, we basically compute the empirical distribution of the simulated quantities to get the distribution of interest. We present our findings for the CRP. In this case $\theta = \theta$, and the corresponding functions are given by

$$p(\mathbf{m}^n | \theta) = \theta^{K^n} \frac{\Gamma(\theta)}{\Gamma(\theta + n)} \prod_{j=1}^{K^n} \Gamma(m_j^n) \quad \text{and} \quad q_k^n(\mathbf{m}^n) = \begin{cases} \frac{m_j^n}{\theta + n}, & k \leq K^n; \\ \frac{\theta}{\theta + n}, & k = K^n + 1. \end{cases}$$

In addition, the the posterior distribution of the number of distinct species to be observed in the enlarged sample of size n^* is given by

$$\Pr(K_{n^*} = k|\theta, \mathbf{m}^n) = \theta^k \frac{(\theta)_n}{(\theta)_{n+n^*}} \sum_{l=k}^{n^*} \binom{m}{l} |s(l, k)| (n)_{m_l}, \quad k = 0, 1, \dots, n^*,$$

where $(a)_n = a(a+1) \dots (a+n-1)$ and $|s(n, k)|$ stands for the sign-less Stirling number of the first kind. Figure 11 displays the posterior distribution of the number of new species in a new sample of $n^* = 50$ individuals using these two approaches. Furthermore, Table 6 shows posterior summaries for these distributions. Notice that in average both methods predict almost the same number of new species to be discovered in a new sample of size 50, although the simulation based approach prediction is a bit higher.

Method	Mean	Median	Sd	Q 2.5%	Q 97.5%
SSM based	11.17	11.00	2.94	6.00	17.00
Lijoi's based	10.62	10.00	2.90	5.00	16.00

Table 6: Posterior summaries for the number of distinct species to be observed in the enlarged sample of size n^* K_{n^*} . Computations based on an extension of the MCMC carried out to perform posterior inference about the parameter θ of a CRP.

6 Discussion

In this work we have offered four detailed case studies that use Bayesian modeling techniques in order to answer complex questions. At every instance, we have provided specifics about model formulation, prior elicitation, simulation-based algorithms computation, and posterior inference. We hope that the reader benefits from such effort and considers the Bayesian paradigm a natural way to solve data-driven problems.

Even though the Bayesian approach to statistical inference is extremely beneficial, some challenges remain. In particular, we recommend consider alternative inference methods in order to account for “big data”, which is currently an active research area in computational statistics (e.g., variational methods). See for example Ormerod and Wand (2010).

References

Banerjee, S., Carlin, B., and Gelfand, A. (2014). *Hierarchical modeling and analysis for spatial data*. Crc Press.

- Gelman, A., Carlin, J., Stern, H., and Rubin, D. (2014). *Bayesian data analysis*, volume 2. Taylor & Francis.
- Jackman, S. (2009). *Bayesian analysis for the social sciences*, volume 846. John Wiley & Sons.
- Lijoi, A., Mena, R. H., and Prünster, I. (2007). Bayesian nonparametric estimation of the probability of discovering new species. *Biometrika*, 94(4):769–786.
- Müller, P., Quintana, F. A., Jara, A., and Hanson, T. (2015). *Bayesian nonparametric data analysis*. Springer.
- Müller, P. and Rodriguez, A. (2013). *Nonparametric Bayesian Inference*. NSF-CBMS regional conference series in probability and statistics. Inst Of Mathematical Stat.
- Ormerod, J. and Wand, M. P. (2010). Explaining variational approximations. *The American Statistician*, 64(2):140–153.
- Pitman, J. (1995). Exchangeable and partially exchangeable random partitions. *Probability theory and related fields*, 102(2):145–158.
- Pitman, J. (1996). Some developments of the blackwell-macqueen urn scheme. *Lecture Notes-Monograph Series*, pages 245–267.
- Prado, R. and West, M. (2010). *Time Series: Modeling, Computation, and Inference*. Chapman and Hall/CRC.
- Robert, C. (2007). *The Bayesian choice: from decision-theoretic foundations to computational implementation*, volume 2. Springer.
- Rodríguez, A. and Quintana, F. A. (2015). On species sampling sequences induced by residual allocation models. *Journal of statistical planning and inference*, 157:108–120.
- Taddy, M. and Kottas, A. (2010). A bayesian nonparametric approach to inference for quantile regression. *Journal of Business & Economic Statistics*, 28(3):357–369.
- Tsay, R. S. (2010). *Analysis of Financial Time Series*. CourseSmart. Wiley.
- West, M. and Harrison, J. (1999). *Bayesian Forecasting and Dynamic Models*. Springer Series in Statistics. Springer New York.

A Notation

The cardinality of a set A is denoted by $|A|$. If P is a logical proposition, then $1_P = 1$ if P is true, and $1_P = 0$ if P is false. $\lfloor x \rfloor$ denotes the floor of x , whereas $[n]$ denotes the set of all integers from 1 to n , i.e., $\{1, \dots, n\}$. The Gamma function is given by $\Gamma(x) = \int_0^\infty u^{x-1} e^{-u} du$.

Matrices and vectors with entries consisting of subscripted variables are denoted by a boldfaced version of the letter for that variable. For example, $\mathbf{x} = (x_1, \dots, x_n)$ denotes an $n \times 1$ column vector with entries x_1, \dots, x_n . We use $\mathbf{0}$ and $\mathbf{1}$ to denote the column vector with all entries equal to 0 and 1, respectively, and \mathbf{I} to denote the identity matrix. A subindex in this context refers to the corresponding dimension; for instance, \mathbf{I}_n denotes the $n \times n$ identity matrix. The transpose of a vector \mathbf{x} is denoted by \mathbf{x}^\top ; analogously for matrices. Moreover, if \mathbf{X} is a square matrix, we use $\text{tr}(\mathbf{X})$ to denote its trace and \mathbf{X}^{-1} to denote its inverse. The norm of \mathbf{x} , given by $\sqrt{\mathbf{x}^\top \mathbf{x}}$, is denoted by $\|\mathbf{x}\|$.